Experimental and theoretical study of band structure of InSe and $In_{1-x}Ga_xSe$ ($x<0.2$) under high pressure: Direct to indirect crossovers

F. J. Manjón,* D. Errandonea,† A. Segura, and V. Muñoz
Departament de Física Aplicada i Institut de Ciència dels Materials de la Universitat de València, C/. Dr. Moliner, 50, 46100 Burjassot, València, Spain

G. Tobías, P. Ordejón, and E. Canadell
Institut de Ciència dels Materials de Barcelona, CSIC, Campus de la UAB, 08193 Bellaterra, Barcelona, Spain

(Received 19 September 2000; published 13 March 2001)

This paper reports on the pressure dependence of the absorption edge of indium selenide and $In_{1-x}Ga_xSe$ alloys ($x<0.2$) up to the pressure at which precursor effects of the phase transition prevent further transmission measurements. The absorption edge could be divided into three components exhibiting different pressure coefficients: one corresponding to a direct transition that could be analyzed through the Elliot-Toyozawa theory, and two supplementary edges with quadratic dependence on the photon energy. The first component is attributed to the direct transition at the Z point of the rhombohedral Brillouin zone. One of the quadratic absorption edges red shifts under pressure and can be attributed to a Z-B indirect transition. The direct transition and the second quadratic edge have a very similar pressure evolution, with a lower pressure coefficient for the latter. This second quadratic edge can be attributed to an indirect transition from an additional maximum of the valence band, which becomes the absolute one under pressure, to the Z conduction-band minimum. Both assignments are in agreement with density-functional theory band-structure calculations also reported in the paper. The three transitions show nonlinear behavior under pressure, which is attributed to the nonlinear evolution of the uppermost valence band at the Z point at low pressures. Above 1 GPa, the three transitions behave almost linearly, with pressure coefficients (in InSe) of 64, 42, and -22 meV/GPa for the direct and indirect transitions, respectively. The strength of the direct transition is shown to be related to the change under pressure of the spin-orbit coupling of the uppermost Se p_z conduction band with lower lying Se p_x-p_y bands. The evolution of the exciton width is also discussed and shown to be governed by the increase of intervalley scattering as a consequence of direct to indirect band-gap crossovers.

DOI: 10.1103/PhysRevB.63.125330 PACS number(s): 78.20.Bh, 71.20.Nr, 71.35.Cc, 78.40.Fy

I. INTRODUCTION

The layered semiconductors of the III-VI family have been studied for several decades due to their special interest for potential applications to nonlinear optics,[1,2] solar energy conversion,[3] and solid-state batteries.[4,5] These materials present an anisotropic structure with layers formed by two deformed sublayers of hexagonal symmetry held together by strong covalent cation-cation bonds along the c axis (perpendicular to the layers). The weaker bonding between the layers is of van der Waals type and leads to the existence of polytypes with different stacking sequences.

Application of pressure allows for a better understanding of the electronic properties of layered semiconductors through the tuning of the anisotropy degree of their chemical bonds and its effect on the optical transitions. The direct gap in InSe,[6–8] GaSe,[9] GaTe,[10] and $In_{1-x}Ga_xSe$ alloys[8] behaves in a nonlinear way under pressure showing a redshift at low pressure, a minimum at a particular pressure, and a blueshift above such pressure. On the other hand, several indirect gaps have been measured in these compounds showing a redshift under pressure with similar pressure coefficients. Those gaps have been attributed to the Γ-M indirect transition in GaSe (Refs. 8 and 11). In GaTe, the indirect transition has not been assigned because of the lack of a reasonable band-structure calculation.[10] The exciton ionization energy in these compounds has been shown to decrease with increasing pressure mainly due to the increase of the dielectric constants for polarizations parallel[12] and perpendicular[9,13–15] to the c axis. Besides, a broadening of the direct exciton line has been observed above certain pressure, which has been attributed to the phonon-assisted intervalley scattering of conduction-band electrons after a direct-indirect band-gap crossover.[7,9,10]

Indium selenide grown by the Bridgman method crystallizes in the γ polytype, which belongs to the space group C_{3v}^5 ($R3m$). InSe has a rhombohedral unit cell and its corresponding first Brillouin zone (BZ) is shown in Fig. 1(a). Despite the early x-ray diffraction measurements showing that InSe grown by the Bridgman method crystallizes in the γ polytype, early band-structure semiempirical pseudopotential calculations were made for β (Ref. 16) and ϵ (Ref. 17) polytypes. The three-dimensional band structure of γ-InSe was calculated only in the last decade through an *ab initio* pseudopotential method[18] and a combined linear muffin-tin orbital (LMTO), atomic sphere approximation (ASA), local-density approximation (LDA) method[19] and, very recently, through a full-potential linearized augmented plane-wave (LAPW) method,[20] yielding very similar results. Calculations of Refs. 18 and 20 include the spin-orbit interaction.

In this work we present measurements of the absorption coefficient of InSe and $In_{1-x}Ga_xSe$ alloys ($x<0.2$) under

 ©2001 The American Physical Society

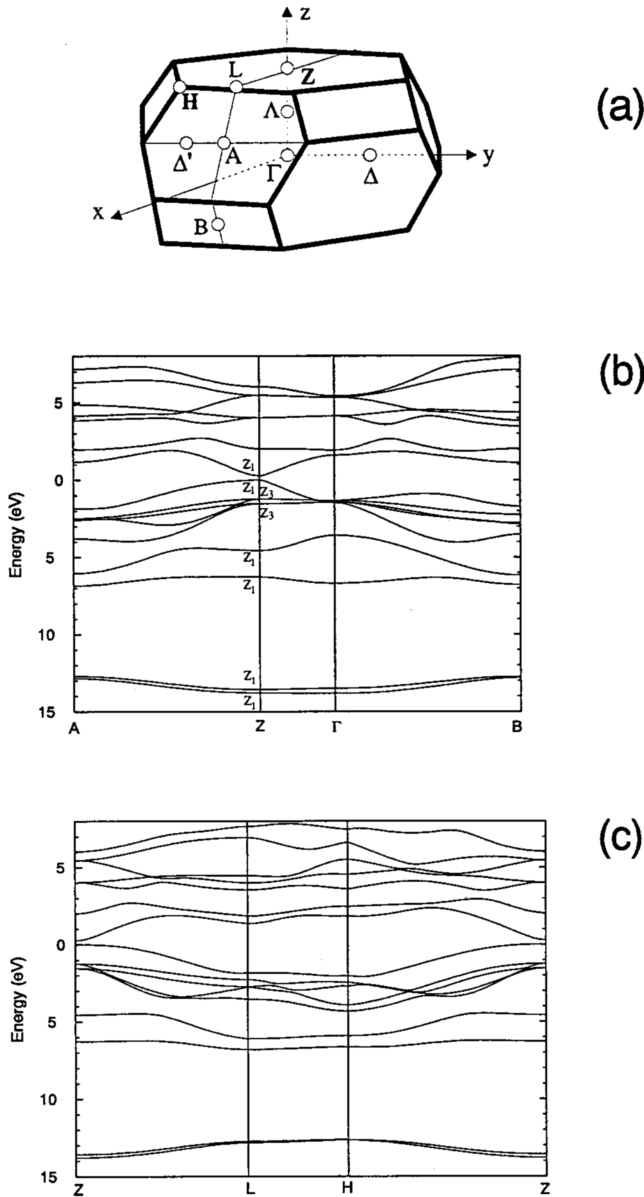

FIG. 1. (a) Rhombohedral Brillouin zone of γ-InSe. (b) Band structure of γ-InSe as calculated through the NAO-DFT method, along the A-Z-Γ-B path. (c) Same as in (b), along the path Z-L-H-Z. In (b) and (c), $E=0$ corresponds to the Fermi energy level.

pressure. Results are interpreted on the basis of numerical atomic orbitals density-functional theory (NAO-DFT) band-structure calculations. The technical aspects of the calculation and the experimental setup are described in Sec. II. Results and discussion are presented in Sec. III. Given the large amount of experimental results, each aspect of them will be presented and discussed in a different subsection of Sec. III. In Sec. IV we present the conclusions of this work.

II. CALCULATION TECHNIQUE AND EXPERIMENT

A. Calculation technique

In this work, we present fully self-consistent density-functional theory[21] (DFT) calculations of the electronic structure of InSe. The calculations are performed in the local-density approximation.[22] The exchange-correlation potential is that of Ceperley and Adler[23] as parametrized by Perdew and Zunger.[24] Only the valence electrons are considered in the calculation, with the core being replaced by norm-conserving scalar relativistic pseudopotentials[25] factorized in the Kleinman-Bylander form.[26] The pseudopotentials were generated using the atomic configurations $4s^2 4p^4$ for Se and $5s^2 5p^1$ for In. The cutoff radii were 1.4, 1.6, 2.0, and 2.0 a.u. for the s, p, d, and f components in selenium, respectively, and 2.5, 2.75, 3.0, and 3.0 a.u. for the s, p, d, and f components of indium, respectively. We also include nonlinear partial-core corrections[27] with matching radii of 1.235 a.u. for Se and 1.9 a.u. for In to describe the exchange and correlation in the core region, since for these elements the core and the valence charges overlap significantly (because the $3d$ and $4d$ electrons of Se and In, respectively, are maintained in the core).

The valence one-particle problem was solved using a linear combination of numerical (pseudo-) atomic orbitals with finite range.[28] The details of the basis generation (including multiple-ζ and polarization functions) can be found in Ref. 29. In this work we have used a split-valence double-ζ basis set with a single shell of polarization orbitals (that is, containing two s shells, two p shells, and one d shell both for Se and for In), as obtained with an energy shift of 250 meV and a split norm of 15%.[29] The integrals of the self-consistent terms of the Kohn-Sham Hamiltonian are obtained with the help of a regular real space grid on which the electron density is projected. The Hartree potential is calculated by means of fast Fourier transforms in that grid. The grid spacing is determined by the maximum kinetic energy of the plane waves that can be represented in that grid. In the present work, we used a cutoff of around 100 Ry (which changes slightly with the volume of the unit cell). A regular grid of $7\times7\times7$ k points[30] was used to sample the BZ. We have checked that the results are well converged with respect to the real space grid, the BZ sampling and the range of the numerical atomic orbitals. The calculations were performed using the SIESTA code.[29,31] For band-structure calculations at high pressures, the lattice parameters were taken from Ref. 22 and the atomic positions inside the cell were assumed to be those proposed in Ref. 32, on the basis of extended x-ray absorption fine-structure (EXAFS) experiments under pressure.

B. Experimental details

Single crystals of γ-InSe and $In_{1-x}Ga_xSe$ alloys ($x<0.2$) have been grown by the Bridgman-Stockbarger method. Thin samples, 10–30 μm in thickness, were cleaved perpendicular to the [001] direction from the ingot and cut into pieces of 100×100 μm in size. For the optical measurements under pressure a sample is placed together with a ruby chip into a 200-μm-diam hole drilled on a 60-μm-thick Inconel gasket and inserted between the diamonds of a membrane-type diamond anvil cell (DAC).[33] A 4:1 methanol-ethanol mixture has been used as pressure-transmitting medium ensuring hydrostatic conditions up to 10 GPa.[34] The pressure has been determined by the calibration method of the ruby luminescence.[35]

For absorption measurements white light from a tungsten lamp was chopped at 180 Hz and focused onto the sample inside the DAC in a 25-μm-diam spot. Transmitted light was again collimated, spatially filtered, and focused on the entrance slit of a 1 m single-grating monochromator used with a bandwidth of 32 Å (0.5 Å for the pressure determination from the ruby luminescence). The light dispersed by the monochromator was detected by a Si or Ge photodiode, the response of which was synchronously measured with a lock-in amplifier. All measurements have been performed at room temperature with incident unpolarized light propagating in the direction perpendicular to the layers.

The transmittance spectra of the samples were measured in the DAC using the sample-in sample-out method[9] up to ~10 GPa. Stray light was measured in the high absorption region of the sample for every spectrum and subtracted from the transmission spectrum. Afterwards, the experimental transmittance spectrum was scaled in order to fit the theoretical value in the spectral range through which the sample is transparent. Finally, the absorption coefficient α was obtained from the scaled transmittance, the sample thickness, and the sample reflectivity. The pressure dependence of both the sample thickness and reflectivity was taken into account. The sample thickness at room pressure has been obtained from the interference fringe pattern in the transparent region and its variation with pressure is calculated from the compressibility of the sample along the c axis.[36] The proportion of Ga in the alloys has been estimated from a linear interpolation of the direct band gap of the samples between those of InSe and GaSe as expected from the linear dependences observed in the a and c axis in $In_{1-x}Ga_xSe$ samples.[37] The pressure dependence of the refractive index of the $In_{1-x}Ga_xSe$ alloys has been interpolated using the refractive indices of InSe and GaSe. The compressibility data of InSe has been used in order to calculate the absorption coefficient of the $In_{1-x}Ga_xSe$ alloys. The pressure dependence of the 4:1 methanol-ethanol mixture refractive index has been obtained from Ref. 38.

III. RESULTS AND DISCUSSION

A. Band structure of γ-InSe

Figures 1(b) and 1(c) show the band structure of γ-InSe calculated with the method described above. In order to compare with previous results, the band structure is shown in two different paths of the rhombohedral BZ. The calculations underestimate the value of the band gap, which is a well-known tendency of the LDA approximation in semiconductors. This could be corrected by using the "scissors operator," as was done in Ref. 18. We have not done so in this work, since we are not interested in a quantitative determination of the band-gap energies, but rather on a qualitative description of the electronic transitions and their pressure dependence. Apart from the differences due to the scissors operator, our results are very close in energy and dispersion to those of Refs. 18–20.

Figure 1(c) shows the band structure in a path in which the change of the wave vector is parallel to the layers. This path gives a much more precise look into the anisotropy of the band structure, in order to compare with optical or transport experimental results, as most of them are made in configurations in which the electric field is parallel or perpendicular to the anisotropy axis. The path used in Fig. 1(b) (and in Refs. 18–20) partially hides the anisotropy, as the electron wave vector in directions Z-A or Z-B has a large component along the c axis. Results in Fig. 1(c) confirm the effective mass "anomaly" that was detected by early empirical pseudopotential band-structure calculations:[16,17] the electron and hole effective masses along the layers are much larger than those along the c axis. This feature of InSe has been confirmed by cyclotron resonance for electrons[39] ($m_{e\perp}/m_{e\parallel}=1.8$) and band-to-acceptor photoluminescence for holes[40] ($m_{h\perp}/m_{h\parallel}=3.5$). Simple $\mathbf{k}\cdot\mathbf{p}$ model considerations explain this effective-mass "anomaly." The reciprocal effective masses at the Z valence-band maximum are given by[41,42]

$$\left[\frac{1}{m_{vZ}^{*}}\right]_{\perp}=1+\frac{2}{m_0}\sum_{k}\frac{|\langle vZ|P_{\perp}|k\rangle|^2}{E_{vZ}-E_k}, \qquad (1)$$

$$\left[\frac{1}{m_{vZ}^{*}}\right]_{\parallel}=1+\frac{2}{m_0}\sum_{k}\frac{|\langle vZ|P_{\parallel}|k\rangle|^2}{E_{vZ}-E_k}, \qquad (2)$$

for wave vectors perpendicular and parallel to the c axis, respectively. $\langle vZ|P_{\perp,\parallel}|k\rangle$ stands for the dipolar matrix element between the valence-band maximum and other extrema at the Z point for light polarization perpendicular and parallel to the c axis. At the Z point the uppermost valence band has predominant Se p_z antibonding character and the lowermost conduction band has predominant In s antibonding character. Both electronic states belong to the Z_1 representation of C_{3v} point group and the transition between them (i.e., the fundamental transition) is fully allowed only for light polarization parallel to the c axis. For light polarization perpendicular to the c axis (parallel to the layers) the fundamental transition is forbidden and it is only weakly allowed because of spin-orbit interaction, which mixes p_z and p_{xy} states belonging to the C_{3v} double group Z_6 representation ($J=\frac{1}{2}$). As the matrix element with the conduction band is very large for light polarization parallel to the c axis,[43] Eq. (2) leads to a negative and small effective mass, which correlates with the large dispersion exhibited by the valence band in the Γ-Z direction. However, for light polarization perpendicular to the c axis, allowed transitions to the Z_1 bands with large matrix elements are those from Z_3 valence bands (with Se p_{xy} character) lying 1 to 1.5 eV below the uppermost valence band and those from Z_3 conduction bands (with In p_{xy} character) lying 4 to 5 eV above the uppermost valence band.[42] As each of these transitions give contributions with different signs in Eq. (1), these contributions compensate each other, leading to a large value of the hole effective mass in the direction parallel to the layers. This large value is coherent with the low dispersion of the valence band in directions Z-L and Z-H, near the Z point.

Comparison with early empirical pseudopotential band-structure calculations[16,17] shows that the interlayer interaction was underestimated in those calculations, which yielded a much narrower uppermost valence band and lowermost

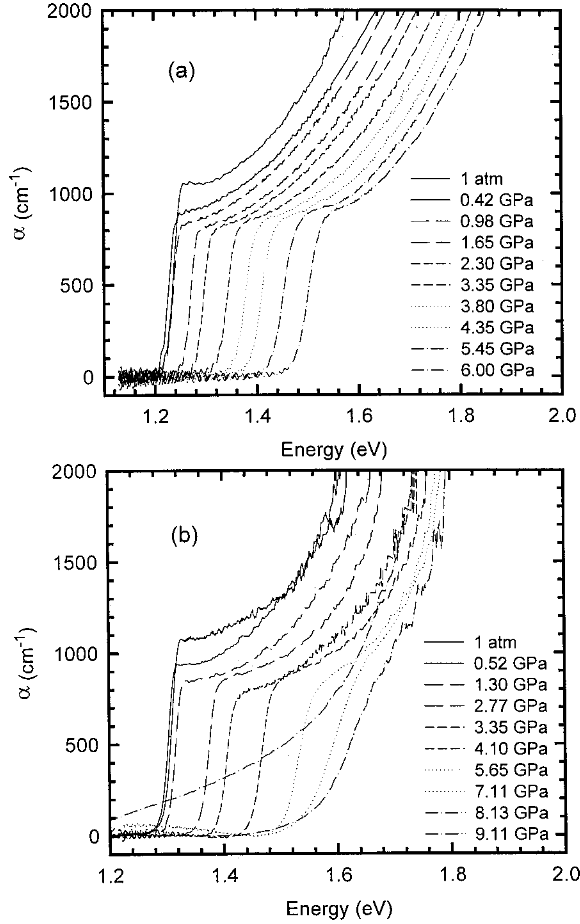

FIG. 2. Room temperature optical absorption spectra of (a) a 18-μm sample of InSe and (b) a 26-μm sample of $In_{0.88}Ga_{0.12}Se$ as a function of pressure.

conduction band. For electron wave vectors in the symmetry planes (directions *Z-A*, *Z-B*, *Z-L*, etc.) the point group of the crystal is C_s and the electronic states belong either to the representations A' or A'' (symmetrical or antisymmetrical with respect to plane reflection, respectively). Compatibility relations between C_{3v} and C_s groups show that Z_1 states become A' and degenerate Z_3 states become A' or A''. The Se p_z A' states mix with Se p_{xy} A' states. This mixing was also clearly underestimated in early calculations,[16,17] yielding an uppermost valence band that remains extremely flat in the layer plane, even far away from the c axis, in contrast with recent calculations (Fig. 1 and Refs. 18–20).

B. Optical absorption coefficient as a function of pressure

Figures 2(a) and 2(b) show the evolution of the fundamental absorption edge of InSe and $In_{0.88}Ga_{0.12}Se$ for light polarization perpendicular to the c axis as a function of pressure, respectively. At low pressures the absorption edge red shifts, reaching a minimum at 0.4, 0.5, and 0.6 GPa in InSe, $In_{0.88}Ga_{0.12}Se$, and $In_{0.81}Ga_{0.19}Se$, respectively (for GaSe the minimum occurs at about 1.3 GPa). Above that pressure range, the fundamental edge shifts towards higher energies. The absorption intensity, which can be inferred from the exciton step structure, also exhibits a minimum around 1.5 GPa and increases for higher pressures. The upper pressure reachable in each sample was limited by the appearance of linear defects, precursors of the transition to the NaCl structure, which strongly scatter the light beam.

The steplike fundamental edge has been analyzed with the Elliott-Toyozawa model for the direct absorption including electron-hole interaction. According to this model, the absorption edge can be described by the analytical expression given by Goñi *et al.*,[44]

$$\alpha_d(E)=C\frac{\sqrt{\mathcal{R}}}{nE}\left\{\sum_{i=1}^{\infty}\frac{2\mathcal{R}}{i^3}\frac{\Gamma_i/2+b(E-E_i)}{(\Gamma_i/2)^2+(E-E_i)^2}+\frac{1}{2}\left[\frac{\pi}{2}-\arctan\left(\frac{E-E_{\mathrm{dg}}}{\Gamma_c/2}\right)\right]-\sum_{i=1}^{\infty}\frac{\mathcal{R}}{i^3}\frac{\Gamma_c/2}{(\Gamma_c/2)^2+(E-E_i)^2}+\frac{\pi}{2}\frac{\sinh(2u^+)}{\cosh(2u^+)-\cos(2u^-)}\right\}, \tag{3}$$

with

$$u^{\pm}=\pi\sqrt{\frac{\mathcal{R}}{2}}\sqrt{\frac{[(E-E_{\mathrm{dg}})^2+(\Gamma_c/2)^2]^{1/2}\pm(E-E_{\mathrm{dg}})}{(E-E_{\mathrm{dg}})^2+(\Gamma_c/2)^2}}, \tag{4}$$

$$E_i=E_{\mathrm{dg}}-\mathcal{R}/i^2, \tag{5}$$

where n is the refractive index, $\mathcal{R}$ is the Rydberg energy, E_{dg} is the direct gap energy, E_i is the energy of the ith exciton line, Γ_i is the width of the ith exciton line, Γ_c is the continuum width, b is the asymmetry parameter of the exciton lines, and C is a parameter that measures the strength of the interaction, which is given by the expression

$$C=\frac{(2\mu)^{3/2}e^2}{\hbar^2 c\varepsilon_0 m_0}\frac{|P|^2}{m_0}, \tag{6}$$

with μ the exciton reduced mass, m_0 the free electron mass, ε_0 the vacuum dielectric constant, and P the matrix element for the electron-photon interaction. For the ith exciton linewidth we have used an empirical relation proposed by Le Toullec, Piccioli, and Chervin:[45]

$$\Gamma_i=\Gamma_c-(\Gamma_c-\Gamma_i)/i^2. \tag{7}$$

Le Toullec, Piccioli, and Chervin[45] showed that the exciton lines at low temperatures exhibit a small asymmetry in GaSe. In order to avoid further parameters whose pressure dependence is not known we have neglected the asymmetry by taking $b=0$ in Eq. (3). In the fitting procedure, we have only considered terms with $i\leqslant 3$ because of the factor i^{-3}. We have also neglected the effect of the band nonparabolicity, which is not known in InSe.

In Fig. 3 we show an example of the analysis of the absorption spectrum of a sample of InSe at 1 atm [Fig. 3(a)] and at 6.8 GPa [Fig. 3(b)]. In these spectra, the fundamental

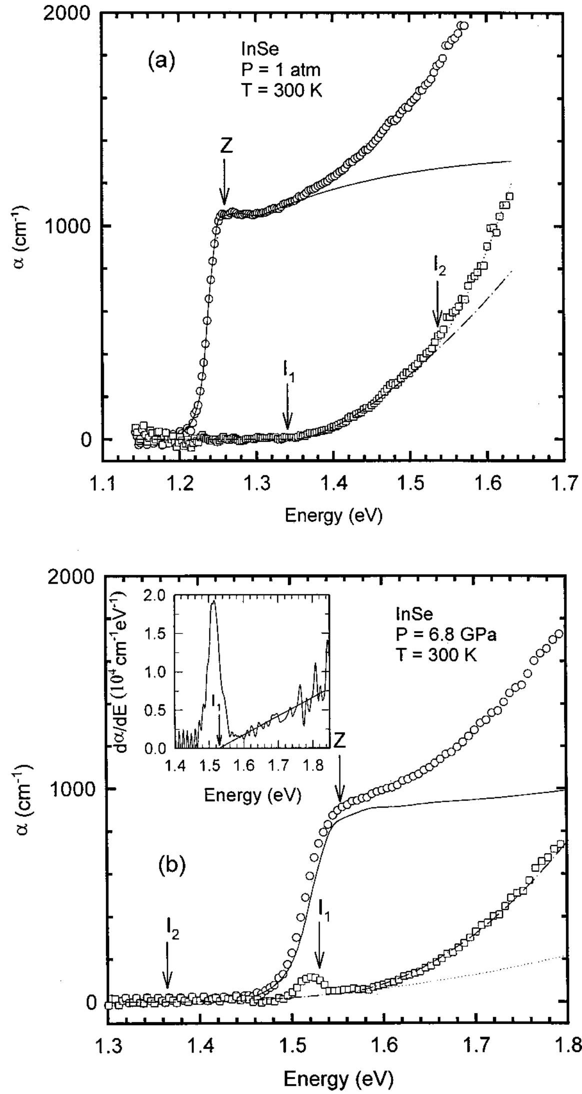

FIG. 3. Experimental and fitted optical absorption spectra of InSe at (a) $P=1$ atm and (b) $P=6.8$ GPa. Experimental data (circles) are fitted by the Elliott-Toyozawa model for the direct gap (solid line). The difference between the experimental data and the theoretical fit is represented by squares and fitted to two indirect absorption edges. The dashed line indicates the contribution of the I_1-Z indirect gap and the dotted line the contribution of the Z-I_2 indirect gap. The positions of the Z direct and I_1 and I_2 indirect gaps at different pressures are indicated by arrows. The inset in (b) shows the first derivative of the absorption coefficient at 6.8 GPa with the position of the I_1 indirect gap.

edge of the absorption coefficient is modeled by Eq. (3). The fitting parameters are the energy (E_1), absorption intensity $[\alpha(E_1)]$ and linewidth (Γ_1) of the ground exciton level, the continuum width (Γ_c), and the exciton Rydberg energy ($\mathcal{R}$). In order to minimize the effects of having the five parameters unconstrained, the evolution of the direct gap energy $E_{\rm dg}$ as a function of pressure has been determined additionally using the first and second derivative of the absorption spectra with respect to the photon energy. A similar evolution of the direct band-gap energy has been obtained from both methods within errors of 5 meV below 4 GPa and 15 meV above 4 GPa (due to the broadening of the absorption edge above this pressure). The inset of Fig. 3(b) illustrates the use of a first-derivative spectrum at 6.8 GPa. Trial values for the band-gap energy and exciton width are given by the peak shape of the derivative spectra, while the extrapolation of the straight line yields an estimation of the indirect absorption edge.

In our analysis, the result of the fit to the Elliott-Toyozawa model has been subtracted from the absorption coefficient, which yields the high-energy tail represented by squares in Fig. 3. This tail was tentatively fitted to a square function of the energy in a previous paper showing an indirect gap with a negative pressure coefficient.[8] A closer study has shown that the complete tail cannot be fitted only with a single quadratic function of the photon energy. Two quadratic functions with different pressure coefficients yield a better fit. The absorption coefficient for photon energies close to the indirect gap energy E_g^i for a dipole-allowed transition with emission of phonons is given by

$$\alpha_i(E)=\begin{cases}\dfrac{A}{E}\left[\dfrac{(E-E_g^i-E_f)^2}{1-\exp(E_f/k_BT)}\right] & \text{for } E>E_g^i+E_f\\ 0 & \text{for } E<E_g^i+E_f\end{cases} \quad (8)$$

if excitonic effects are neglected. A is a constant proportional to the matrix element of the transition and E_f is the energy of the phonon involved in the transition. The phonon absorption was neglected in the analysis, as it mainly contributes to the low absorption tail, which could not be measured with such thin samples. It must be remarked that the decomposition procedure is subject to errors in the pressure ranges through which the three absorption edges are nearly resonant. Also, the absolute intensity of the indirect absorption edges resulting from this procedure may be affected by the fact that the band nonparabolicity was not taken into account in the Elliot-Toyozawa model. In spite of these cautionary statements, the fact that each component of the absorption edge has a different pressure behavior and the coherent trend exhibited by these components as a function of the gallium content of the alloy provides us with strong evidence for the physical basis of the decomposition. It must also be remarked that very similar results are obtained from photoluminescence experiments under pressure.[46]

C. Pressure dependence of the direct and indirect band-gap energies

Figure 4 shows the pressure dependences of the direct and indirect edges in InSe and $In_{0.88}Ga_{0.12}Se$ that result from the fitting procedure described in the previous subsection. We will refer to the quadratic edges of low and high onset energy as I_1 and I_2, respectively.

In InSe and in $In_{1-x}Ga_xSe$, the three transitions show nonlinear pressure dependences at low pressures and almost linear behaviors above 2 GPa. A similar nonlinear behavior of the band gaps has also been observed in GaSe (Ref. 9) and GaTe (Ref. 10). In InSe, the three transitions behave almost linearly above 2 GPa with pressure coefficients of 62, 42, and -22 meV/GPa for the Z, I_1, and I_2 transitions, respectively. The energy differences between the I_1 and I_2 indirect

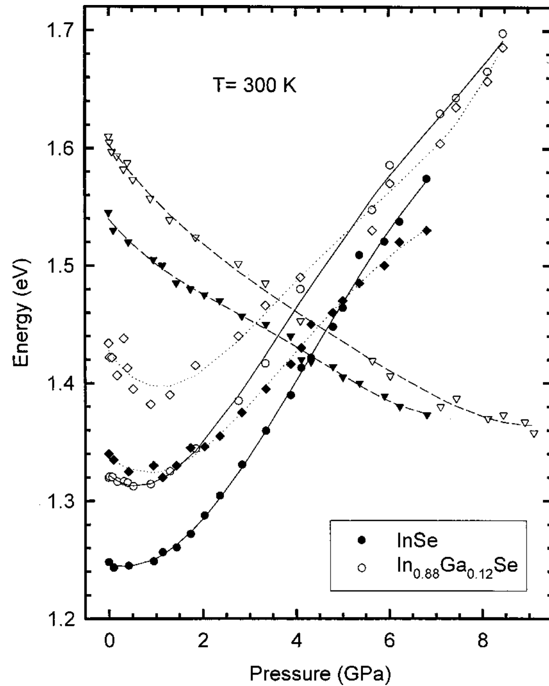

FIG. 4. Pressure dependence of the direct and indirect gaps in InSe (filled symbols) and $In_{0.88}Ga_{0.12}Se$ (hollow symbols). The direct gap position at the Z point of the BZ is represented by circles, the I_1 indirect edge by rhombohedrals, and the I_2 indirect edge is symbolized by triangles.

edges with respect to the Z direct gap show an almost linear pressure dependence, with pressure coefficients of -76 ± 10 meV/GPa and -19 ± 5 meV/GPa for the Z-I_2 and I_1-Z energy differences, respectively, as shown in Fig. 5.

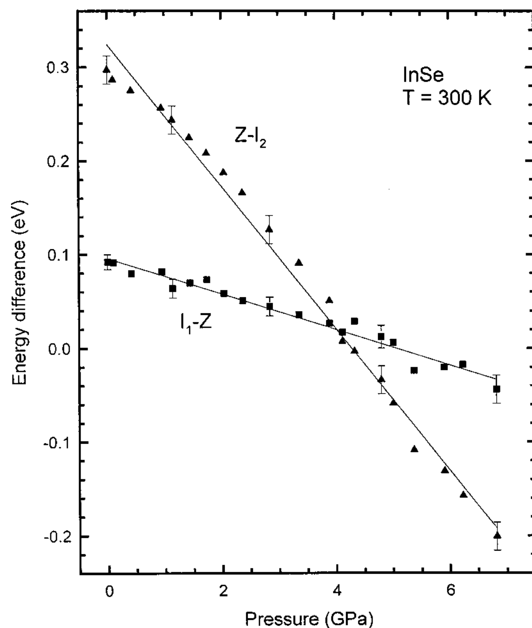

FIG. 5. Experimental pressure dependence of the energy separation between the I_1 (squares) and I_2 (triangles) indirect edges with respect to the Z direct gap. Solid lines are the fits of the data to linear equations on pressure.

With respect to the direct gap, our experimental results basically agree with those of other authors.[6,7,8,19,20] According to the band structures shown in Figs. 1(b) and 1(c) this absorption edge corresponds to a direct transition at the Z point, which is weakly allowed due to the to the spin-orbit contribution of Se p_x-p_y states to a band with predominant Se p_z character. In the NAO-DFT band structure shown in Figs. 1(b) and 1(c) the spin-orbit interaction was not taken into account. This fact accounts for the low dispersion of the Se p_z valence band near the Z point in direction Z-L as discussed above.

Regarding the quadratic absorption edges, I_2 is located 0.3 eV above the direct gap in InSe at ambient pressure and was already reported by Errandonea *et al.*[8] with a similar pressure dependence. Its existence was also suggested, from transport measurements in Ref. 44. It should also be noted that its pressure dependence scales with that of the Γ-M indirect edge in GaSe.[9] The observation of the indirect edge I_1, located 70 meV above the direct edge in InSe at ambient pressure, is proposed here for the first time.

Let us discuss the assignment of these quadratic absorption edges. Two nonequivalent minima exist in the conduction band of InSe, at points A and B of the BZ, which are located above the absolute minimum at the Z point of the BZ at zero pressure. The A and B minima are triply degenerate, with the B minima closer in energy to the Z minimum [Fig. 1(b)]. Under pressure, both minima shift down in energy, but the B minima remain lower in energy and shifts down with a higher pressure coefficient. Figure 6(a) shows the evolution of the band structure in the region of the band gap for different pressures, as calculated through the NAO-DFT method in the H-Z-B path of the BZ [Fig. 1(a)]. Figure 6(b) shows the evolution of three band gaps marked in Fig. 4 as a function of pressure. Above 2 GPa, the pressure coefficients of the direct, ZH to Z, and Z to B transitions are 68, 41, and -13 meV/GPa, respectively. For comparison with experimental results of Fig. 5, we show in the insert of Fig. 6(b) the calculated energy differences between the indirect transitions and the direct one. The calculated pressure coefficient of the energy difference between the Z to B indirect transition and the Z direct transition is -89 meV/GPa (average value from 0 to 7 GPa), which is very close to the experimental value of the Z-I_2 energy difference (-76 ± 10 meV/GPa). The agreement is remarkably good if we obtain the calculated pressure coefficient between 3 and 7 GPa (-76.6 meV/GPa). This result is not surprising because the experimental pressure coefficient for the Z-I_2 gap was determined mainly from the pressure range above 3 GPa in which the indirect gap energy is obtained with lower errors from the fitted spectra. Table I summarizes the comparison between experimental and theoretical pressure coefficients. From these results, the assignment of the I_2 indirect edge to a Z-B indirect transition seems quite well founded.

Regarding the I_1 edge, results of Figs. 6(a) and 6(b) and Table I give also the key for the assignment. This indirect edge would correspond to an indirect transition from the valence-band maximum that develops under pressure (both in the K-L and K-H directions) to the conduction-band minimum at the Z point of the BZ. It must be remarked that

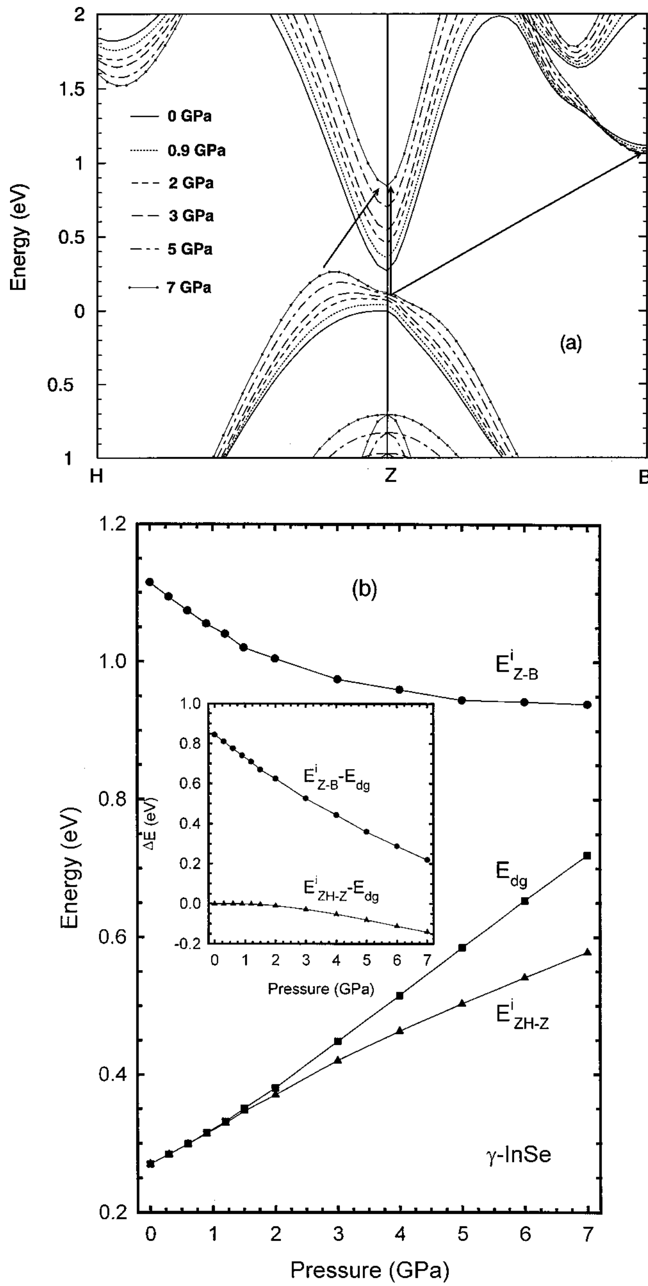

FIG. 6. (a) Detail of the band structure of InSe in the *H-Z-B* path as calculated through a NAO-DFT method at different pressures. (b) Theoretical variation under pressure of the three transitions to which the observed direct and indirect transitions are assigned. The inset in (b) shows the theoretical pressure dependence of the energetic separation between the I_1 (squares) and I_2 (triangles) indirect edges with respect to the Z direct gap.

in β-InSe or ε-InSe band structures calculated through empirical pseudopotential methods,[16,17] the absolute maximum of the valence band was found to be in the Γ-K direction. Nevertheless, no strong experimental evidence of this indirect gap was found. In most previous claims of having observed this indirect gap, the proposed values for the indirect edge were just below the direct gap in an interval of photon energies in which a quadratic edge can be masked by the exciton low-energy tail. The first strong experimental evidence of a direct-indirect band-gap crossover in InSe was given by the pressure behavior of the exciton width at low temperature.[7] The calculated pressure coefficient of the energy difference between the *ZH* to Z indirect transition and the Z direct transition, as calculated through the NAO-DFT method, is -20 meV/GPa (average value from 0 to 7 GPa). This result is in good agreement with the experimental value of the I_1-Z energy difference (-19 ± 5 meV/GPa) and supports the assignment of the I_1 indirect edge to the *ZH* to Z transition.

The previous discussion about the hole effective mass along the layers, based in Eq. (1), suggests an interpretation of the appearance of these maxima: NAO-DFT band-structure calculations show that the energy difference between Z_3 in p_{xy} conduction bands and the uppermost valence band increases under pressure, whereas the energy difference between the uppermost valence band and the Z_3 Se p_{xy} valence bands decreases under pressure (inset of Fig. 8). This means that the negative terms in Eq. (1) ($\mathbf{k}\cdot\mathbf{p}$ interaction with Z_3 conduction bands) decrease in absolute value and the positive terms ($\mathbf{k}\cdot\mathbf{p}$ interaction with Z_3 valence bands) increase under pressure, resulting in a positive curvature for the uppermost valence band at Z above a certain pressure, which would shift the maximum of the band away from the Z point.

Figures 6(a) and 6(b) are not conclusive about the existence of extra maxima in the valence band at ambient pressure. It must be remembered that the spin-orbit interaction was not taken into account in the calculation. As this interaction mixes Se p_z and p_{xy} states with Z_6 double group symmetry ($J=\frac{1}{2}$), the maximum at the Z point is expected to remain under pressure. In the pressure range through which only an increase of the band flatness is observed in Fig. 6(a), an alternative interpretation is possible. In this range, the I_1 quadratic edge would be a nonparabolic contribution to the direct absorption edge, getting stronger and starting closer to it as the *ZH* maxima develop under pressure. Nevertheless, experimental results on stimulated photoluminescence under pulsed excitation and especially the behavior of the band-gap renormalization strongly suggest the existence of additional maxima in the valence band even at low pressure: band-gap renormalization and the quasi-Fermi-level energy are correlated only if a large proportion of photoexcited carriers are "hidden" in extra reservoir extrema.[46]

It must be stressed again that the energy difference between the I_1 and I_2 indirect gaps with respect to the Z direct gap shows an almost linear pressure dependence (Fig. 5). This linear pressure dependence between the Z minimum and the B minima energy difference corresponds with results of transport measurements under pressure in InSe (Ref. 47) that show a deep level becoming deeper with pressure with a pressure coefficient similar to that of the Z-I_2 energy difference. The linear fits in Fig. 5 suggest that in InSe the I_1 indirect edge would be located 96 ± 8 meV higher than the Z direct gap and the pressure coefficient of the I_1-Z energy difference would be -19 ± 5 meV/GPa, whereas the I_2 indirect edge would be located 325 ± 15 meV above the Z direct gap and the pressure coefficient of the Z-I_2 energy difference would be -76 ± 10 meV/GPa. Table II summarizes the

TABLE I. Comparison between experimental and theoretical pressure coefficients in InSe. E_{dg} represents the direct gap energy at Z and E_x^i corresponds to the different x indirect gaps.

Experiment		Theory	
$\frac{\partial E_{dg}}{\partial P}$ (meV/GPa) ($P>2$ GPa)	62 ± 5	$\frac{\partial E_{dg}}{\partial P}$ (meV/GPa) ($P>2$ GPa)	68
$\frac{\partial E^i_{I_1}}{\partial P}$ (meV/GPa) ($P>2$ GPa)	42 ± 5	$\frac{\partial E^i_{ZH-Z}}{\partial P}$ (meV/GPa) ($P>2$ GPa)	42
$\frac{\partial E^i_{I_2}}{\partial P}$ (meV/GPa) ($P>2$ GPa)	-22 ± 5	$\frac{\partial E^i_{Z-B}}{\partial P}$ (meV/GPa) ($P>2$ GPa)	-13
$\frac{\partial(E^i_{I_1}-E_{dg})}{\partial P}$ (meV/GPa)	-19 ± 10	$\frac{\partial(E^i_{ZH-Z}-E_{dg})}{\partial P}$ (meV/GPa)	-28
$\frac{\partial(E^i_{I_2}-E_{dg})}{\partial P}$ (meV/GPa)	-76 ± 10	$\frac{\partial(E^i_{Z-B}-E_{dg})}{\partial P}$ (meV/GPa)	-89

experimental energy differences observed in several alloys of different composition between their direct and indirect transitions at zero pressure. From Table II, we note that the pressure coefficient of the Z-I_2 separation increases with Ga content of the samples. The pressure coefficient of the Z-I_2 separation is -80 meV/GPa for $x=0.07$ and -94 meV/GPa for $x=0.19$. An extrapolation of these results to $x=1$ indicates that the M minima in GaSe would be 10 ± 20 meV above the Γ minimum and that the pressure coefficient of the Z-I_2 energy difference would be -105 ± 15 meV/GPa. Both values are in agreement with the values reported for GaSe in literature.[9]

As the indirect edges here reported correspond to the energy of the indirect gap plus a phonon, if we assume the phonon energy to be about 25 meV, an estimation of the direct-indirect crossover pressures is possible. In Table II the values of the Z-I_2 direct-indirect crossover pressures for the different compounds studied are summarized. From these data we obtain that the Z-B crossover pressure depends linearly on the Ga proportion, x_{Ga}, according to the equation:

$$P_c=(4.1\pm0.2)-(3.9\pm0.6)x_{Ga}. \quad (9)$$

with P_c expressed in GPa. If we extrapolate this result to $x_{Ga}=1$ we obtain that the equivalent to the Z-B crossover would occur in GaSe (within errors) almost at room pressure. This result is in agreement with the observation of the M indirect edge slightly below the Γ direct edge in GaSe at room pressure.[9] The I_1-Z crossover is estimated to occur at 3.5 ± 0.2 GPa in InSe and in the alloys (independently of the gallium concentration, in the range of compositions here studied).

Let us now discuss the nonlinear behavior of all transitions in the low-pressure range. It should be first pointed out that NAO-DFT calculations here reported do not reproduce the nonlinear behavior shown in Fig. 4 for all transitions. This may be related to the inability of the local-density approximation to describe correctly essentially nonlocal interactions, such as van der Waals interactions, which dominate in the low-pressure range of compression. This is an open and important theoretical research subject.

In previous works[7,9] the nonlinear pressure dependence of the direct band gap in InSe and GaSe was interpreted through phenomenological models in terms of intralayer and interlayer deformation potentials, the former accounting for a bonding-antibonding *intralayer positive* contribution and the latter accounting for a band splitting or widening *interlayer negative* contribution. The interlayer contribution is predominant at low pressure, due to the stronger initial compression of the interlayer distance as compared to the intralayer distances. A quantitative account of the band-gap pressure dependence could be given with one intralayer and one interlayer deformation potential. Those models, first proposed by Gauthier *et al.*,[9] are based on the assumption that all intralayer distances vary under pressure as the a parameter does, i.e., the layer compression is isotropic and the intralayer bond angles do not change under pressure. Recent EXAFS measurements in GaSe (Ref. 48), InSe (Ref. 32), and GaTe (Ref. 49) have shown that this assumption cannot be maintained. In fact, the layer ''thickness'' (the in-layer Se-Se distance along the c axis) slightly increases in the low-

TABLE II. Values of the crossover pressure (P_C) of direct and indirect edges, opacity pressure (P_O), and I_1-Z and Z-I_2 differences at room pressure in InSe and $In_{1-x}Ga_xSe$ ($x<0.2$) alloys.

X (% Ga)	P_C (GPa)	P_O (GPa)	$\Delta E(I_1$-$Z)$ (meV)	$\Delta E(Z$-$I_2)$ (meV)
0.00	4.3	6.5	96 ± 8	325 ± 15
0.07	4.1	7.8	94 ± 10	300 ± 10
0.12	3.9	9.1	110 ± 10	290 ± 10
0.16	3.8	7.6	103 ± 10	270 ± 10
0.19	3.5	9.3	100 ± 10	265 ± 10

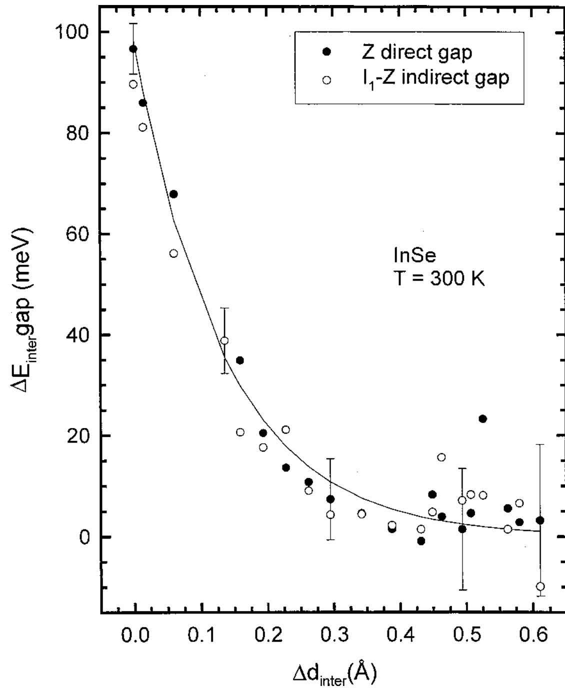

FIG. 7. Pressure dependence of the interlayer contribution to the evolution of the Z direct and I_1-Z indirect gaps in InSe at room temperature. The line represents the fit of experimental data for the direct gap to the Eq. (10).

pressure range and, consequently, the interlayer distances turn out to decrease under pressure much quicker than assumed in Refs. 7 and 9. Using the pressure behavior of the interlayer and intralayer distances obtained in Ref. 32, the nonlinear behavior of the direct and indirect gaps in InSe cannot be reproduced with such a simple intralayer and interlayer deformation potential model. Even if the model is modified in order to redefine the intralayer deformation potential as a function of In-In bond length, the dramatic change of the interlayer distance under pressure prevents from any quantitative fit with simply two numbers.

The almost linear pressure dependence of the direct and indirect gaps in InSe above 2 GPa suggests the possibility that the nonlinear effect of interlayer forces becomes negligible above that pressure. The interlayer deformation potential would be strongly pressure dependent. In order to estimate the evolution of the interlayer contribution to the direct and indirect gaps as a function of pressure, we can extrapolate the linear dependence of the gaps above 2 GPa to room pressure and plot the difference between the pressure evolution of the gaps and that of their high-pressure linear dependence, $\Delta E_{\mathrm{inter}}(P)$, as a function of the variation of the interlayer distance, $\Delta d_{\mathrm{inter}}(P)$, given in Ref. 32. Figure 7 represents the evolution of the nonlinear component of the Z direct and I_1-Z indirect gaps in InSe as a function of the interlayer distance. The pressure dependence of the nonlinear component can be fitted to an exponential law given by

$$\Delta E_{\mathrm{inter}}(P)=\Delta E_{\mathrm{inter}}(0)\exp[-\Delta d_{\mathrm{inter}}(P)/d_0], \qquad (10)$$

where d_0 is a distance representing the range of the nonlinear contribution. Using the high-pressure linear coefficients of the Z direct gap and I_1 indirect gap (62 and 42 meV/GPa in InSe, respectively), we could calculate the low-pressure nonlinear contribution of Z and I_1-Z gaps and its pressure dependence. Fits of data of Fig. 7 to Eq. (10) yield the following values: $\Delta E_{\mathrm{inter}}(0)=0.098(7)$ eV and $d_0=0.133(4)$ Å for the Z direct gap and 0.089(4) eV and 0.132(7) for the I_1-Z indirect gap. Both results indicate a very similar contribution of the interlayer interaction to the direct and indirect gaps in agreement with previous reasonings. Poorer results (not shown in Fig. 7) were obtained for the Z-I_2 indirect gap due to the bigger errors in the determination of the position of the I_2 minima at low pressures, as previously commented. Results on interlayer distances under pressure in GaSe given in Ref. 50 have been also analyzed with Eq. (10), yielding values of $\Delta E_{\mathrm{inter}}(0)=0.197(3)$ eV and $d_0=0.181(4)$ Å for the Γ direct gap and 0.239(5) eV and 0.188(2) Å for the Γ-M indirect gap by taking the pressure linear coefficients of 61 and -41 meV/GPa for the Γ and Γ-M gaps, respectively. These results indicate that (i) the nonlinear interlayer contribution to the pressure behavior of the band gaps is bigger in GaSe than in InSe and (ii) the variation of this contribution decreases more rapidly in InSe than in GaSe, as indicated by the lower values of d_0 in InSe. The nonlinear contribution of the interlayer interaction becomes negligible for a decrease of the interlayer distance of 0.2 Å in InSe and 0.4 Å in GaSe. A plausible interpretation of this behavior would consider that d_0 represents the range of the interlayer distance decrease through which van der Waals forces dominate the interlayer interaction, whereas beyond that range, strong interlayer repulsion forces would dominate and give a linear contribution.

D. Strength of the direct absorption as function of pressure

Figure 8 shows the pressure dependence of the C parameter (absorption intensity or strength) of Eq. (3) for polarization $\mathbf{E}\perp\mathbf{c}$ in InSe, as obtained from the absorption coefficient at the steplike contribution of the direct gap. A very similar dependence has been found in $\mathrm{In}_{1-x}\mathrm{Ga}_x\mathrm{Se}$ ($x<0.2$) samples. The occurrence of a minimum of intensity could in principle be correlated to the pressure evolution of the direct gap. Nevertheless, the minimum of C occurs at a higher pressure with respect to that of the direct gap. If the direct transition for the polarization $\mathbf{E}\perp\mathbf{c}$ were fully allowed, one would expect $C \propto E_{\mathrm{dg}}^{3/2}$, corresponding to a pressure-independent matrix element as observed in GaAs.[44] The increase of the matrix element above 2 GPa in InSe contrasts with the behavior observed in GaSe (Ref. 9) and GaTe (Ref. 10) in which the matrix element decreases in the pressure range between 0 and 4 GPa.

The behavior of the direct absorption strength C could be understood if we consider that the fundamental direct transition for polarization $\mathbf{E}\perp\mathbf{c}$ in the III-VI layered materials is only weakly allowed by spin-orbit interaction, as discussed by several authors.[7,9,10,52] In this sense, the pressure dependence of the absorption intensity of the direct gap would depend inversely on the distances between the topmost valence band (with Z_1 character) and the lower-lying valence bands with Z_3 character through a spin-orbit coupling term.

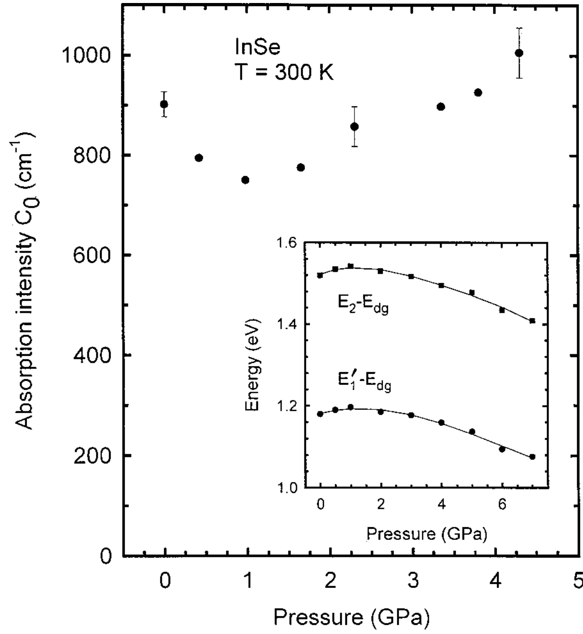

FIG. 8. Strength of the direct transition for the **E**⊥ **c** polarization as function of pressure. Solid circles indicate the pressure evolution of the C parameter of the Elliott-Toyozawa model calculated assuming a constant Rydberg energy above 4 GPa. A similar evolution but with a smaller pressure coefficient is observed when an increase of the Rydberg energy is assumed above 2 GPa. The solid line indicates the expected behavior of the interband matrix element for a spin-orbit allowed transition in InSe according to Eq. (10). The inset figure shows the energetic separation between the p_x-p_y valence bands with respect to the topmost p_z valence band at Z.

This means that the larger the separation between the Z_1 and Z_3 valence bands the smaller the spin-orbit coupling and consequently the smaller the strength of the direct fundamental transition for polarization **E**⊥ **c**.

Kuroda, Munakata, and Nishina[53] applied Hopfield's quasicubic model[54] and deduced the spin-orbit splitting (ΔE_0) and the crystal-field anisotropy (ΔE_c) from the energy differences between bands with p_z and p_x-p_y anion character at point Z of the BZ. Within Hopfield's model the matrix element ($P_\perp$) of the direct transition for the polarization **E**⊥ **c** in this scheme is given by the expression[53]

$$P_\perp^2 = \tfrac{2}{3} P_0^2 \left(\frac{2\Delta E_0}{3\Delta E_c} \right)^2, \tag{11}$$

where P_0 is the matrix element for the allowed transition whose typical value is 20 eV. This interpretation of the value of the direct transition can be accepted with some reservation because available band-structure calculations for InSe (Refs. 14, 16, and Sec. II A in this work) show that the energy difference between the anion nonbonding p_z band and the p_{xy} bands at Z are mainly due to the strong dispersion of the p_z band in the Γ-Z direction. Strictly speaking, it should be considered as a crystal-field anisotropy splitting only at the Γ point. In fact, at the Γ point, where Hopfield's model should be applied, band-structure calculations with spin-orbit interaction[18,20] show a much stronger mixing between Γ_6 bands ($J=\frac{1}{2}$) with p_z and p_{xy} character, as these bands are much closer in energy to each other with respect to their relative situation at the Z point.

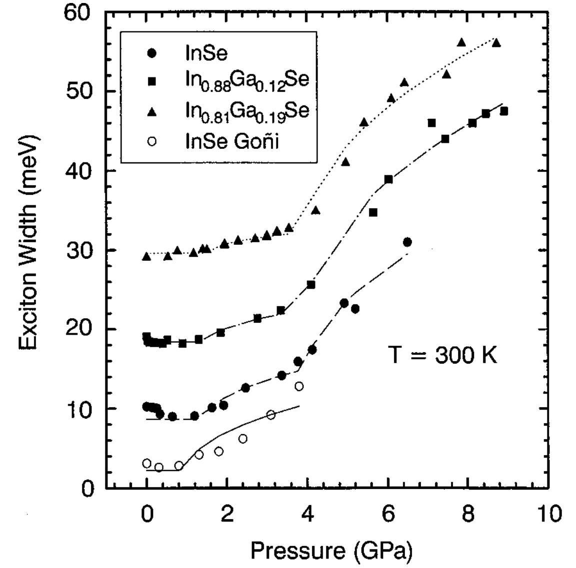

FIG. 9. Exciton linewidth as function of pressure in InSe, $In_{0.88}Ga_{0.12}Se$, and $In_{0.81}Ga_{0.19}Se$. Linewidths have been shifted in 0.1 eV for the sake of clarity. Open symbols represent the pressure dependence of the linewidth obtained by Goñi *et al.* at 10 K in InSe (after Ref. 7). Lines represent the fits of Eq. (12) to the experimental data.

In spite of these reservations, it seems reasonable to assume that the contribution of the Se p_x-p_y valence bands to the valence-band maximum at Z (with predominant p_z character), is inversely proportional to the energy difference between both types of bands. These energy differences, $E_2 - E_{dg}$ and $E_1' - E_{dg}$, have been obtained in InSe through absorption[6] and photoreflectance measurements under pressure[19,20] and are shown in the inset of Fig. 8. This figure shows an increase of the separation of the p_z and p_x-p_y bands up to 1.5 GPa and a decrease above that pressure, which is perfectly coherent with the proposed interpretation. This explanation also agrees well with the behavior of the matrix element observed in GaSe,[9] in which the energy separation ΔE_{v12} increases up to 4 GPa.[6] Even if the pressure dependence of higher-energy direct transitions in GaTe is not known, a similar behavior is expected, given the fact that the minimum of the fundamental gap occurs at a much higher pressure.[10]

E. Pressure dependence of the direct exciton and continuum widths

Figure 9 shows the pressure dependence of the exciton linewidth for samples of InSe and $In_{1-x}Ga_xSe$ ($x<0.2$) at room temperature. The behavior observed in the three samples is similar with an almost constant value of the exciton linewidth at low pressure and a progressive reversible broadening of the exciton line above 1.5 GPa. Goñi *et al.* reported a similar evolution of the exciton linewidth at 10 K, increasing for pressures above 1 GPa (Ref. 7) (hollow sym-

bols in Fig. 9). Such a broadening of the exciton line has been observed, for example, in GaAs above 4.2 GPa, and has been interpreted as a result of phonon-assisted intervalley scattering of conduction-band electrons between the direct and indirect minima of the conduction band,[44] when the Γ-X direct-indirect crossover occurs. A similar broadening has been observed in GaSe (Ref. 9) and GaTe (Ref. 10) above 0 and 1 GPa, respectively. The broadening of the direct exciton led Goñi *et al.* to suggest the presence of an indirect gap close to the direct one in InSe at zero pressure.[7] This result is coherent with the conduction-band structure proposed in this work, provided one assumes that around 1 GPa the direct exciton at Z is scattered to indirect excitonic levels associated with the indirect transition between the ZH maxima of the valence band [Fig. 6(a)] and the Z maximum of the valence band. As those maxima would be located some 50 meV below the Z maximum at 1 GPa, if we assume that the indirect process occurs via emission of a phonon of $\sim$25 meV, the ionization energy of the indirect exciton associated to the new maxima would be about 40 meV. Given the complex structure of the valence band at these pressures, simple effective-mass models are not in principle adapted for an interpretation of this experimental estimate of the indirect exciton binding energy.

It seems also reasonable to attribute the further increase of the linewidth above 4 GPa to the Z-I_2 band-gap crossover. In order to give account of results of Fig. 9 we use a simple model of intervalley electron scattering (via deformation potential) in the effective mass approximation.[55] We assume that the intervalley deformation potential is independent of the phonon mode and the exciton homogeneous linewidth is given by

$$\Gamma_{\mathrm{exc}}=\frac{\hbar}{2}(P_i+P_{Z1}+P_{Z2}), \tag{12}$$

where P_{Z1} and P_{Z2} are the probabilities of intervalley scattering from the Z maximum to the I_1 maxima of the valence band and from the Z minimum to the I_2 minima of the conduction band, respectively, and P_i is the contribution of inhomogeneous processes and defect scattering to the total exciton linewidth. According to Conwell, the intervalley scattering probability is given by

$$P_{Zi}=\frac{N_i m_i^{3/2} D_{Zi}^2}{\sqrt{2}\pi\hbar^2\rho E_q}[(n_q+1)(\Delta E_{Zi}-E_q)^{1/2}+n_q(\Delta E_{Zi}+E_q)^{1/2}], \tag{13}$$

where the first term corresponds to intervalley scattering with phonon emission and the second term corresponds to the phonon absorption process. $N_1=3$ and $N_2=3$ are the number of equivalent indirect minima in the conduction band, m_i is the density-of-states effective mass at the i minima, $\rho=5.53\ \mathrm{g/cm^3}$ is the material density, E_q and n_q are the phonon energy and the occupation, respectively, ΔE_{Zi} is the energy difference between the Z direct valley and the indirect valleys and D_{Zi} is the intervalley deformation potential.

Assuming that the I_1-Z direct-indirect crossover is the responsible for the broadening of the direct exciton linewidth above 1 GPa (with a pressure coefficient for ΔE_{ZI_1} of -19 meV/GPa) and that the Z-I_2 direct-indirect crossover is the responsible for the additional broadening of the direct exciton linewidth above 4 GPa (with a pressure coefficient for ΔE_{ZI_2} of -76 meV/GPa), we estimate the deformation potential for the I_1-Z (D_{Z1}) and Z-I_2 (D_{Z2}) intervalley scattering to be $D_{Z1}=13\pm3$ eV/Å and $D_{Z2}=6.3\pm2.0$ eV/Å in InSe, $D_{Z1}=11\pm3$ eV/Å and $D_{Z2}=7.2\pm2.0$ eV/Å in $In_{0.88}Ga_{0.12}Se$ and $D_{Z1}=9\pm3$ eV/Å and $D_{Z2}=7.5\pm2.0$ eV/Å in $In_{0.81}Ga_{0.19}Se$. For this estimates we have assumed an energy of $\sim$25 meV for the phonon involved in both I_1-Z and Z-I_2 scattering processes. We think that the lower value $D_{Z1}=6\pm2$ eV/Å obtained by Goñi *et al.* in InSe (Ref. 7) is due to the much higher pressure coefficient of ΔE_{Zi} used by these authors.

Finally, we want to mention that the evolution of the continuum width with pressure in the studied samples showed a similar behavior to that of the linewidth of the direct exciton. This result gives no additional information for the continuum width evolution and confirms that the same scattering of electrons and holes of the direct exciton affect the electrons and holes of the direct gap.

IV. CONCLUSIONS

We have studied the band structure of InSe and $In_{1-x}Ga_xSe$ ($x<0.2$) alloys at room temperature by means of absorption measurements under pressure and NAO-DFT band-structure calculations. The measured absorption edge shows multicomponent character that has been assigned to one direct and two indirect optical transitions involving different points of the Brillouin zone, whose direct and indirect energy gaps have been determined as a function of pressure. By comparison with the calculated electronic band structure at several pressures, the indirect transition that blueshifts under pressure has been assigned to a transition between additional maxima of the valence band along the Z-H direction and the conduction-band minimum at the Z point. This interpretation is in agreement with the reversible broadening of the direct exciton linewidth observed in absorption measurements above 1.5 GPa in InSe (and at similar pressures in the $In_{1-x}Ga_xSe$ alloys here studied) caused by the direct-indirect Z-ZH band-gap crossover of the valence band. This broadening of the direct exciton linewidth was already noted by Goñi *et al.* in InSe above 1 GPa.[7] Furthermore, our interpretation is also in agreement with the reversible broadening of the direct band-to-band photoluminescence linewidth observed above 1.2 GPa in InSe, which will be presented elsewhere.[56] In a similar way, the indirect transition that redshifts under pressure has been assigned to a transition between the Z maximum of the valence band and the B minima of the conduction band. This interpretation is in agreement with the abrupt reversible decrease of the intensity of the photoluminescence, corresponding to the direct band-to-band recombination, which is observed above 4 GPa in InSe due to the direct-indirect Z-B band-gap crossover of the conduction

band.[11,56] Furthermore, this interpretation is also in agreement with the reversible broadening of the direct exciton linewidth observed in absorption measurements above 4 GPa in InSe and $In_{1-x}Ga_xSe$ alloys.

It must be stressed that in the $In_{1-x}Ga_xSe$ ($x<0.2$) alloys the pressures for the direct-indirect Z-I_2 band-gap crossover vary linearly with the Ga concentration between InSe and GaSe. In contrast, the pressure for the I_1-Z direct-to-indirect band-gap crossover has been found to be independent of the cation composition. This latter result is in agreement with the expected anionic nature of the topmost valence band.

The three optical transitions studied in this work in InSe and $In_{1-x}Ga_xSe$ alloys present a nonlinear behavior of the band-gap energies upon application of pressure. Similar nonlinear behavior has been reported in previous works for the direct gaps of InSe,[7,8] GaSe,[9] and GaTe.[8,10] The nonlinear contribution to the band-gap energies in InSe, which decreases considerably above 2 GPa (also for $In_{1-x}Ga_xSe$ alloys here studied), has been shown to decrease exponentially with the interlayer distance. Above 2 GPa, linear pressure coefficients of 62, 42, and −22 meV/GPa have been measured for the Z, I_1, and I_2 transitions, respectively. On the other hand, the analysis of the absorption edge of the direct transition has revealed that the strength of the direct transition for the polarization $\mathbf{E}\perp\mathbf{c}$ evolve under pressure in close correlation with the energy separation of the Se p_z upper valence band and the lower-lying Se p_x-p_y bands, mixed by spin-orbit interaction. This result is in qualitative agreement with the model proposed by Kuroda, Munakata, and Nishina to explain the matrix element of the direct transition in the III-VI layered materials[53] and with the experimentally observed behavior of the matrix element of the direct transition in GaSe.[9]

Finally, some words must be said regarding structural stability. InSe and GaSe samples undergo a structural phase transition to the NaCl structure above 10.5 and 25 GPa, respectively.[36,48,51] However, precursor effects of the phase transition have been observed above 7 and 19 GPa in InSe and GaSe, respectively, through the appearance of defects that make samples opaque to visible radiation. Table II shows the different values of the opacity pressures observed in InSe and $In_{1-x}Ga_xSe$ ($x<0.2$) alloys. Those values indicate that the more the gallium concentration on the samples the more stables samples become. This feature is in complete agreement with the higher stability of GaSe with respect to InSe.

In summary, the use of hydrostatic pressure in combination with first-principles calculations has allowed us to obtain a picture of the electronic band structures of InSe and $In_xGa_{1-x}Se$ alloys and the change of its basic interactions upon reduction of the lattice parameters. The combination of experimental hydrostatic pressure and theoretical first-principles calculations has been revealed as a powerful method for a better understanding of complicated band structures, such as those of the III-VI layered semiconductor compounds.

ACKNOWLEDGMENTS

One of the authors, F.J.M., wants to express his gratitude to C. Ulrich for providing LMTO band structure calculations of the III-VI layered materials, and to K. Syassen, N. E. Christensen, and A. R. Goñi for their help. F.J.M. also acknowledges economical support from Generalitat Valenciana. Part of this work was supported by the DGES–Spain Project PB96-0859 and by Generalitat de Catalunya (1999 SGR 207). P.O. acknowledges support from Fundacion Ramon Areces (Spain). The computations described in this work were carried out using the resources of CESCA and CEPBA coordinated by C4.

*Corresponding author. Present address: Applied Physics Department, Technical University of Valencia, EPSA, Pl. Ferrándiz i Carbonell, E-03800 Alcoy, Alicante, Spain. Electronic mail: Francisco.Manjon@uv.es

†Present address: Hochdruckgruppe, MPI für Chemie, Postfach 3060, D-55020 Mainz, Germany.

[1] R. S. Putnam and D. G. Lancaster, Appl. Opt. **38**, 1513 (1999).

[2] R. A. Kaindl, F. Eickemeyer, M. Woerner, and T. Elsaesser, Appl. Phys. Lett. **75**, 1060 (1999).

[3] J. P. Martinez, A. Segura, J. L. Valdes, and A. Chevy, J. Appl. Phys. **62**, 1477 (1987).

[4] C. Julien, M. Jouanne, P. A. Burret, and M. Balkanski, Solid State Ionics **28–30**, 1167 (1988).

[5] M. Balkanski, P. Gomes da Costa, and R. F. Wallis, Phys. Status Solidi B **194**, 175 (1996).

[6] N. Kuroda, O. Ueno, and Y. Nishina, J. Phys. Soc. Jpn. **55**, 581 (1986).

[7] A. R. Goñi, A. Cantarero, U. Schwarz, K. Syassen, and A. Chevy, Phys. Rev. B **45**, 4221 (1992).

[8] D. Errandonea, F. J. Manjón, J. Pellicer, A. Segura, and V. Muñoz, Phys. Status Solidi B **211**, 33 (1999).

[9] M. Gauthier, A. Polian, J. M. Besson, and A. Chevy, Phys. Rev. B **40**, 3837 (1989).

[10] J. Pellicer-Porres, F. J. Manjón, A. Segura, V. Muñoz, C. Power, and J. González, Phys. Rev. B **60**, 8871 (1999).

[11] F. J. Manjón, Y. van deVijver, A. Segura, V. Muñoz, Z. X. Liu, and C. Ulrich, Phys. Status Solidi B **211**, 105 (1999).

[12] D. Errandonea, A. Segura, V. Muñoz, and A. Chevy, Phys. Rev. B **60**, 15 866 (1999).

[13] N. Kuroda, O. Ueno, and Y. Nishina, Phys. Rev. B **35**, 3860 (1987).

[14] A. Polian, J. M. Besson, M. Grimsditch, and H. Vogt, Phys. Rev. B **25**, 2767 (1982).

[15] F. J. Manjón, Y. van der Vijver, A. Segura, and V. Muñoz, Semicond. Sci. Technol. **15**, 806 (2000).

[16] A. Bourdon, A. Chevy, and J. M. Besson, in *Physics of Semiconductors 1978*, Proceedings of the 14th International Conference of the Physics of Semiconductors, edited by B. L. H. Wilson, IOP Conf. Proc. No. 43 (Institute of Physics and Physical Society, London, 1979), p. 1371.

[17] Y. Depeursinge, Nuovo Cimento Soc. Ital. Fis., B **64**, 111 (1981).

[18] P. Gomes da Costa, R. G. Dandrea, R. F. Wallis, and M. Balkanski, Phys. Rev. B **48**, 14 135 (1993).

[19] C. Ulrich, A. R. Goñi, K. Syassen, O. Jepsen, A. Cantarero, and V. Muñoz, in *Proceedings of the 15th AIRAPT and 33 EHPRG*

Conference, Warsaw, Poland, 1995, edited by W. A. Trzeciakowski (World Scientific, Singapore, 1996), p. 647.

[20] C. Ulrich, D. Olguin, A. Cantarero, A. R. Goñi, K. Syassen, and A. Chevy, Phys. Status Solidi B **221**, 777 (2000).

[21] P. Hohemberg and W. Kohn, Phys. Rev. **136**, 864 (1964).

[22] W. Kohn and L. J. Sham, Phys. Rev. **140**, 1133 (1965).

[23] D. M. Ceperley and B. J. Adler, Phys. Rev. Lett. **45**, 566 (1980).

[24] S. Perdew and A. Zunger, Phys. Rev. B **32**, 5048 (1981).

[25] N. Troullier and J. L. Martins, Phys. Rev. B **43**, 1993 (1991).

[26] L. Kleinman and D. M. Bylander, Phys. Rev. Lett. **48**, 1425 (1982).

[27] S. G. Louie, S. Froyen, and M. L. Cohen, Phys. Rev. B **26**, 1738 (1982).

[28] O. F. Sankey and D. J. Niklewski, Phys. Rev. B **40**, 3979 (1989).

[29] E. Artacho, D. Sanchez-Portal, P. Ordejón, A. Garcia, and J. M. Soler, Phys. Status Solidi B **215**, 809 (1999).

[30] H. J. Monkhorst and J. D. Pack, Phys. Rev. B **13**, 5188 (1976).

[31] D. Sanchez-Portal, P. Ordejón, E. Artacho, and J. M. Soler, Int. J. Quantum Chem. **65**, 453 (1997).

[32] J. Pellicer-Porres, A. Segura, A. San Miguel, and V. Muñoz, Phys. Rev. B **60**, 3757 (1999).

[33] R. Le Toullec, J. P. Pinceaux, and P. Loubeyre, High Press. Res. **1**, 77 (1988).

[34] G. J. Piermarini, S. Block, and J. D. Barnett, J. Appl. Phys. **44**, 5377 (1973).

[35] G. J. Piermarini, S. Block, J. D. Barnett, and R. A. Forman, J. Appl. Phys. **46**, 2774 (1975).

[36] U. Schwarz, A. R. Goñi, K. Syassen, A. Cantarero, and A. Chevy, High Press. Res. **8**, 396 (1991).

[37] A. Gouskov, J. Camassel, and L. Gouskov, Prog. Cryst. Growth Charact. **5**, 323–413 (1982).

[38] J. H. Eggert, L. Xu, R. Che, L. Chen, and J. Wang, J. Appl. Phys. **72**, 2453 (1992).

[39] E. Kress-Rogers, R. J. Nicholas, J. C. Portal, and A. Chevy, Solid State Commun. **44**, 379 (1982).

[40] Ch. Ferrer-Roca, A. Segura, M. V. Andres, J. Pellicer, and V. Munoz, Phys. Rev. B **55**, 6981 (1997).

[41] E. O. Kane, J. Phys. Chem. Solids **1**, 249 (1957).

[42] N. Kuroda and I. Nishina, Physica B **105**, 30 (1980).

[43] N. Piccioli, R. Le Toullec, F. Bertrand and J. C. Chervin, J. Phys. (France) **42**, 1129 (1981).

[44] A. R. Goñi, A. Cantarero, K. Syassen and M. Cardona, Phys. Rev. B **41**, 10 111 (1990).

[45] R. Le Toullec, N. Piccioli, and J. C. Chervin, Phys. Rev. B **22**, 6162 (1980).

[46] F. J. Manjón, A. Segura and V. Muñoz, High Press. Res. **18**, 81 (2000).

[47] D. Errandonea, A. Segura, J. F. Sanchez-Royo, V. Munoz, P. Grima, A. Chevy, and C. Ulrich, Phys. Rev. B **55**, 16 217 (1997).

[48] J. P. Itié, A. Polian, M. Gauthier, and A. San Miguel, ESRF Highlights 1996/1997, (unpublished).

[49] J. Pellicer-Porres, A. Segura, V. Muñoz and A. San Miguel, Phys. Rev. B **61**, 125 (2000).

[50] J. Pellicer-Porres, Ph.D. Thesis, University of Valencia (1999). (unpublished)

[51] K. J. Dunn and F. P. Bundy, Appl. Phys. Lett. **36**, 709 (1980).

[52] J. Camassel, P. Merle, H. Mathieu, and A. Gouskov, Phys. Rev. B **19**, 1060 (1979).

[53] N. Kuroda, I. Munakata, and Y. Nishina, Solid State Commun. **33**, 687 (1980).

[54] J. J. Hopfield, J. Phys. Chem. Solids **15**, 97 (1960).

[55] A. R. Goñi and K. Syassen, in *Semiconductors and Semimetals*, edited by T. Suski and W. Paul (Academic, New York, 1998), Vol. 54, pp. 247–425.

[56] F. J. Manjón, A. Segura, and V. Muñoz (unpublished).